

Global geometric entanglement in transverse-field XY spin chains: finite and infinite systems

Tzu-Chieh Wei

*Department of Physics and Astronomy,
University of British Columbia, Vancouver, BC V6T 1Z1, Canada*

Smitha Vishveshwara

*Department of Physics and Institute for Condensed Matter Theory,
University of Illinois at Urbana-Champaign, Urbana, Illinois 61801, U.S.A.*

Paul M. Goldbart

*Department of Physics, Institute for Condensed Matter Theory,
and Federick Seitz Materials Research Laboratory,
University of Illinois at Urbana-Champaign, Urbana, Illinois 61801, U.S.A.*

Abstract

The entanglement in quantum XY spin chains of arbitrary length is investigated via the geometric measure of entanglement. The emergence of entanglement is explained intuitively from the perspective of perturbations. The model is solved exactly and the energy spectrum is determined and analyzed in particular for the lowest two levels for both finite and infinite systems. The overlaps for these two levels are calculated analytically for arbitrary number of spins. The entanglement is hence obtained by maximizing over a single parameter. The corresponding ground-state entanglement surface is then determined over the entire phase diagram, and its behavior can be used to delineate the boundaries in the phase diagram. For example, the field-derivative of the entanglement becomes singular along the critical line. The form of the divergence is derived analytically and it turns out to be dictated by the universality class controlling the quantum phase transition. The behavior of the entanglement near criticality can be understood via a scaling hypothesis, analogous to that for free energies. The entanglement density vanishes along the so-called disorder line in the phase diagram, the ground space is doubly degenerate and spanned by two product states. The entanglement for the superposition of the lowest two states is also calculated. The exact value of the entanglement depends on the specific form of superposition. However, in the thermodynamic limit the entanglement density turns out to be independent of the superposition. This proves that the entanglement density is insensitive to whether the ground state is chosen to be the spontaneously Z_2 symmetry broken one or not. The finite-size scaling of entanglement at critical points is also investigated from two different view points. First, the maximum in the field-derivative of the entanglement density is computed and fitted to a logarithmic dependence of the system size, thereby deducing the correlation length exponent for the Ising class using only the behavior of entanglement. Second, the entanglement density itself is shown to possess a correction term inversely proportional to the system size, with the coefficient being universal (but with different values for the ground state and the first excited state, respectively).

PACS numbers: 03.67.Mn, 03.65.Ud, 64.70.Tg, 05.70.Jk

I. INTRODUCTION

Entanglement has been recognized in the past decade as a useful resource in quantum information processing [1–4]. Very recently, it has emerged as an actor on the nearby stage of quantum many-body physics, especially for systems that exhibit quantum phase transitions [5–11], where it can play the role of a diagnostic of quantum correlations. Quantum phase transitions [12] are transitions between qualitatively distinct phases of quantum many-body systems, driven by quantum fluctuations. It is conventionally defined as the non-analyticity in the ground-state energy [12]. In view of the connection between entanglement and quantum correlations, one anticipates that entanglement will furnish a dramatic signature of the quantum critical point as the ground-state wavefunction itself should also exhibit certain non-analyticity, which thereby manifests in the singularity of correlations. To describe the ground state usually requires exponentially many parameters, and therefore to detect the non-analyticity hidden in the wavefunction may require an ingenious design of observables. Ground-state energy is usually such a good indicator but it may fail to exhibit singularity, for example, near the isotropic antiferromagnetic point in the XXZ model [13], where there is a continuous transition. Entanglement is thus expected to be an alternative, useful quantity in assisting the determination of quantum phase transitions, complementing traditional methods. On the other hand, the more entangled a state is, usually, though not necessarily, the more useful it is likely to be a resource for quantum information processing [14]. It is thus desirable to study and quantify the degree of entanglement near quantum phase transitions. By employing entanglement to diagnose many-body quantum states one may obtain fresh insight into the quantum many-body problem [5].

To date, progress in characterizing and quantifying entanglement has taken place greatly in the domain of bi-partite systems, and much understanding has been gained in the multi-partite settings, although a complete picture has not yet been achieved [15]. Much of the previous work on entanglement in quantum phase transitions has been based on bi-partite measures, i.e., focus has been on entanglement either between pairs of parties [6, 7, 16] or between a part and the remainder of a system [8–10, 17, 18]. For multi-partite systems, however, the complete characterization of entanglement requires the consideration of multi-partite entanglement, for which a consensus measure has not yet emerged.

Singular and scaling behavior of entanglement near quantum critical points was discov-

ered in important work by Osterloh and co-workers [7], who invoked Wootters' *bi-partite* concurrence [19] as a measure of entanglement. The success of the use of concurrence has been understood via its connection to two-point correlation functions and the derivative of ground-state energy [20]. The drawback of concurrence is that it can deal with only two spins (each with spin-1/2) even though the system may contain an infinite number of spins. Although attempts have been made to generalize concurrence to many spin-1/2 systems via the time reversal operation, the generalized concurrence loses its connection to the entanglement of formation [21]. Furthermore, the use of concurrence may give rise to spurious transition points [22].

Another approach is to consider the von Neumann entropy of a subsystem of L spins with the rest $N - L$ spins of the system. It is found that for critical spin chains the entropy scales logarithmically with the subsystem size L for $N \rightarrow \infty$, with a prefactor that is related to the central charge of the corresponding conformal theory [8–10]. The entanglement addressed in this case is only between a subsystem and the rest of the system, and the connection to central charge is interesting.

A different approach without using entanglement is to consider fidelity or overlap between two different ground-state wavefunctions, which is now called fidelity measure. Non-analytic behavior in the fidelity measure is expected for system parameters close to critical points. This approach has been shown to be successful [23].

Recently, Barnum and co-workers [11] have developed an entanglement measure, which they call generalized entanglement. Instead of using subsystems they use different algebras and generalized coherent states to define the entanglement. They have also applied the generalized entanglement to systems exhibiting quantum phase transitions. Their approach opens a new approach to multi-partite entanglement. Nevertheless, there is no *a priori* choice of which algebra, amongst all possible ones, is the most natural one to use.

In addition to spin chains other models that have been studied by using either the von Neumann entropy (also known as entanglement entropy) or the concurrence as the entanglement measure include: (i) the super-radiance model, in which many two-level atoms interact with a single-mode photon field [24]; and (ii) the one-dimensional extended Hubbard model, in which electrons can hop between the nearest neighbors and there are Coulomb interactions among electrons on the same site and with nearest-neighbor electrons as well [25]. Furthermore, in addition to spin systems, entanglement entropy has been examined in both bosonic

and fermionic systems [18, 26] and the area law (or the breaking of it) has been investigated. In view of other approaches that connect quantum information ideas to condensed matter settings (or vice versa), Verstraete and co-workers [27] have defined an entanglement length, viz., the distance at which two sites can establish a pure-state entanglement at the cost of measuring all other sites. They found that this entanglement length is lower bounded the correlation length. All these, including the theme of the present paper, are aimed at approaching many-body problems from different, and hopefully fresh, perspectives, and at complementing traditional statistical-physical approaches.

In the present paper, we expand and extend results of Ref. [28]. We apply the *global* geometric measure that we have developed in Ref. [29], based on a geometric picture [30–33]; it provides a *holistic*, rather than bi-partite, characterization of the entanglement of quantum many-body systems. Our focus is on one-dimensional spin systems, specifically ones that are exactly solvable and exhibit quantum criticality. The geometric measure has been applied to many models in one dimension [34–38] as well as two dimensions [39] and seems to become a useful tool as well. For these systems, it is found that entanglement behaves in a singular manner near the quantum critical points. This supports the view that entanglement—the non-factorization of wave functions—reflects quantum correlations. This will be explained in detail using the transverse-field XY models as an specific example.

The remaining structure of the present paper is as follows. In Sec. II, we introduce the geometric measure of entanglement (or in short, geometric entanglement) that we shall use to quantify the entanglement of a many-body state. In Sec. III, we introduce the spin XY models in a transverse field, the focus of present paper. We explain in an elementary way the emergence of entanglement away from critical points, so as to expect the drastic behavior of entanglement near criticality. In Sec. IV, we diagonalize the Hamiltonian, invoking Jordan-Wigner and Bogoliubov transformations. We carefully explain the boundary conditions placed on the spin and hence the fermionic operators. In Sec. V, we derive the overlap of the lowest two levels with an Ansatz product state, the result of which is the basis for deriving entanglement for these two states, including the true ground state. Section VI contains the main results of the present paper. We present the results of ground-state entanglement over the entire phase diagram. In Sec. VIA, we illustrate the entanglement results for finite systems. In Sec. VIB, we derive the expression of entanglement for infinite systems. There, the divergence of ground-state entanglement is analyzed and the connection

to the universality classes is established. In Sec. VI C, we show the vanishing of entanglement along the disorder line by demonstrating the ground space is doubly degenerate and spanned by two product states. In Sec. VI D, we discuss the issue of entanglement superposition, and argue the irrelevance of spontaneous symmetry breaking in the determination of ground-state entanglement density. In Sec. VI E, we study the issue of finite-size effect to the entanglement density at criticality. Finally, we summarize in Sec. VII, and give a generic picture of how entanglement behaves near criticality, using a scaling hypothesis. How the geometric entanglement serves to detect non-analyticity of ground-state wavefunction is also discussed.

II. GLOBAL GEOMETRIC MEASURE OF ENTANGLEMENT

We quickly review the global measure that we shall use in the present paper. Consider a general, n -partite, normalized pure state: $|\Psi\rangle = \sum_{p_1 \dots p_n} \Psi_{p_1 p_2 \dots p_n} |e_{p_1}^{(1)} e_{p_2}^{(2)} \dots e_{p_n}^{(n)}\rangle$. If the parties are all spin-1/2 then each can be taken to have the basis $\{|\uparrow\rangle, |\downarrow\rangle\}$. Our scheme for analyzing the entanglement involves considering how well an entangled state can be approximated by some unentangled (normalized) state (e.g., the state in which every spin points in a definite direction): $|\Phi\rangle \equiv \otimes_{i=1}^n |\phi^{(i)}\rangle$. The proximity of $|\Psi\rangle$ to $|\Phi\rangle$ is captured by their overlap; the entanglement of $|\Psi\rangle$ is revealed by the maximal overlap [29–33, 40]

$$\Lambda_{\max}(\Psi) \equiv \max_{\Phi} |\langle \Phi | \Psi \rangle|; \quad (1)$$

the larger Λ_{\max} is, the less entangled is $|\Psi\rangle$. (Note that for a product state, Λ_{\max} is unity.) If the entangled state consists of two separate entangled pairs of subsystems, Λ_{\max} is the product of the maximal overlaps of the two. Hence, it makes sense to quantify the entanglement of $|\Psi\rangle$ via the following *extensive* quantity [41]

$$E_{\log_2}(\Psi) \equiv -\log_2 \Lambda_{\max}^2(\Psi), \quad (2)$$

This normalizes to unity the entanglement of EPR-Bell and N -party GHZ states, as well as giving zero for unentangled states. Finite- N entanglement is interesting in the context of quantum information processing. To characterize the properties of the quantum critical point we use the thermodynamic quantity \mathcal{E} defined by

$$\mathcal{E} \equiv \lim_{N \rightarrow \infty} \mathcal{E}_N, \quad (3a)$$

$$\mathcal{E}_N \equiv N^{-1} E_{\log_2}(\Psi), \quad (3b)$$

where \mathcal{E}_N is the *entanglement density*, i.e., the entanglement per particle.

For translation invariant state, it is shown that the entanglement is either completely in a product state or is globally entanglement [42]. Therefore, the above quantification of entanglement by comparing to product states makes a natural choice.

We remark that by appropriate partitioning of $|\phi\rangle$ into various product forms, a hierarchy of entanglement can be obtained [43, 44]. This hierarchical geometric measure has recently also been applied to the XY model [45, 46]. One can generalize the form of product states, e.g., to a product of blocks of two spins (or multiple spins), and then calculate the entanglement per block [36]. In fact, this approach enables the connection of the spatial renormalization group (RG) (i.e., coarse-graining) procedure to the geometric measure, and the entanglement under RG can be properly defined [37].

III. QUANTUM XY SPIN CHAINS AND EMERGENCE OF ENTANGLEMENT

We consider the family of models governed by the Hamiltonian

$$\mathcal{H}_{XY} = - \sum_{j=1}^N \left(\frac{1+r}{2} \sigma_j^x \sigma_{j+1}^x + \frac{1-r}{2} \sigma_j^y \sigma_{j+1}^y + h \sigma_j^z \right), \quad (4)$$

where r measures the anisotropy between x and y couplings, h is the transverse external field, lying along the z -direction, and we impose periodic boundary conditions, namely, a ring geometry. At $r = 0$ we have the isotropic XY limit (also known as the XX model) and at $r = 1$, the Ising limit. All anisotropic XY models ($0 < r \leq 1$) belong to the same universality class, i.e., the Ising class, whereas the isotropic XX model belongs to a different universality class. XY models exhibit three phases (see Fig. 4): oscillatory, ferromagnetic and paramagnetic. In contrast to the paramagnetic phase, the first two are ordered phases, with the oscillatory phase being associated with a characteristic wavevector, reflecting the modulation of the spin correlation functions (see, e.g., Ref. [47]). We shall see that the global entanglement detects the boundaries between these phases, and that the universality class dictates the behavior of entanglement near quantum phase transitions.

Before we solve the entanglement of the XY model, we give perturbative analysis of, as an illustration of how entanglement arises and vanishes, the Ising model in a transverse field

(viz. $r = 1$)

$$\mathcal{H} = - \sum_{i=1}^N (\sigma_i^x \sigma_{i+1}^x + h \sigma_i^z). \quad (5)$$

At $h = 0$ the ground state is that with all spins pointing up in the x -direction $|\rightarrow\rightarrow\cdots\rightarrow\rangle$ or down $|\leftarrow\leftarrow\cdots\leftarrow\rangle$, which is manifestly unentangled. The ground state can be any superposition of $(|\rightarrow\rightarrow\cdots\rightarrow\rangle$ and $|\leftarrow\leftarrow\cdots\leftarrow\rangle$) when the Z_2 symmetry is not spontaneously broken. For example, the states $(|\rightarrow\rightarrow\cdots\rightarrow\rangle \pm |\leftarrow\leftarrow\cdots\leftarrow\rangle)/\sqrt{2}$ are actually the two lowest levels obtained from solving the models using Jordan-Wigner and Bogoliubov transformations and they both have $E_{\log_2} = 1$. (For small h the entanglement rises quadratically in the case of unbroken symmetry instead of quartically, as we shall show shortly.) We shall see later that whether or not we use a broken-symmetry state has no effect in the thermodynamic limit. For small h (i.e., $h \ll 1/\sqrt{N}$) one can obtain the ground state by treating the $h\sigma_i^z$ terms as perturbations. Take the ground state at $h = 0$ to be $|\rightarrow\rightarrow\cdots\rightarrow\rangle$. Then first-order perturbation theory for the ground state gives

$$\frac{1}{\sqrt{1 + \frac{Nh^2}{16}}} \left(|\rightarrow\rightarrow\cdots\rightarrow\rangle + \frac{h}{4} \sum_i |\rightarrow\cdots\leftarrow_i\cdots\rightarrow\rangle \right). \quad (6)$$

Using the method described in Ref. [29] we obtain $E_{\log_2} \lesssim Nh^2/(16 \ln 2)$ to leading order in h . At $h = \infty$ the ground state is a quantum paramagnet with all spins aligning along the external field: $|\uparrow\uparrow\cdots\uparrow\rangle$, and once more is unentangled. To $\mathcal{O}(1/h)$ perturbation theory gives (treating $\sigma_i^z \sigma_{i+1}^z$ terms small)

$$\frac{1}{\sqrt{1 + \frac{N}{16h^2}}} \left(|\uparrow\uparrow\cdots\uparrow\rangle + \frac{1}{4h} \sum_i |\uparrow\cdots\downarrow_i\downarrow_{i+1}\cdots\uparrow\rangle \right), \quad (7)$$

for which $E_{\log_2} \lesssim N/(16h^2 \ln 2)$, to leading order of $1/h$. The quantum phase transition from a ferromagnetic to a paramagnetic phase occurs at $h = 1$ [12]. The two lowest levels, which we denote by $|\Psi_{1/2}\rangle$ and $|\Psi_0\rangle$ (for reasons to be explained later) are, respectively, the ground and first excited states, and they are asymptotically degenerate for $0 \leq h \leq 1$ when $N \rightarrow \infty$.

IV. DIAGONALIZATION OF THE HAMILTONIAN

As is well known [12, 47, 49], the energy eigenproblem for the XY spin chain can be solved via a Jordan-Wigner transformation, through which the spin degrees of freedom are

recast as fermionic ones, followed by a Bogoliubov transformation, which diagonalizes the resulting quadratic Hamiltonian.

The Jordan-Wigner transformation that we shall make from spins (σ 's) to fermion particles (c 's) is

$$\sigma_i^z = 1 - 2c_i^\dagger c_i, \quad (8a)$$

$$\sigma_i^x = \prod_{j=1}^{i-1} (1 - 2c_j^\dagger c_j) (c_i + c_i^\dagger), \quad (8b)$$

$$\sigma_i^y = -i \prod_{j=1}^{i-1} (1 - 2c_j^\dagger c_j) (c_i - c_i^\dagger). \quad (8c)$$

One has to pay attention to the boundary conditions that are to be imposed on the c 's. Although periodic in the σ 's, one cannot simply take

$$\sigma_{N+1}^x = \prod_{j=1}^N (1 - 2c_j^\dagger c_j) (c_{N+1} + c_{N+1}^\dagger) = \sigma_1 = (c_1 + c_1^\dagger), \quad (9)$$

and conclude that either (i) $\prod_{j=1}^N (1 - 2c_j^\dagger c_j) = 1$ and $c_{N+1} = c_1$, or (ii) $\prod_{j=1}^N (1 - 2c_j^\dagger c_j) = -1$ and $c_{N+1} = -c_1$, neither of which are correct if one wishes to obtain the correct spectrum and eigenstates for arbitrary finite N . Instead one should impose that (as the $(N + 1)$ -th site is identified as the first site)

$$\sigma_N^x \sigma_{N+1}^x = \sigma_N^x \sigma_1^x, \quad (10)$$

which then leads to

$$(c_N + c_N^\dagger)(c_{N+1} + c_{N+1}^\dagger) = - \prod_{j=1}^N (1 - 2c_j^\dagger c_j) (c_N + c_N^\dagger)(c_1 + c_1^\dagger). \quad (11)$$

The two possible conditions that satisfy this are either (I) $\prod_{j=1}^N (1 - 2c_j^\dagger c_j) = -1$ and $c_{N+1} = c_1$, or (II) $\prod_{j=1}^N (1 - 2c_j^\dagger c_j) = 1$ and $c_{N+1} = -c_1$. The operator

$$\prod_{j=1}^N (1 - 2c_j^\dagger c_j) = e^{i\pi \sum_j c_j^\dagger c_j} \quad (12)$$

counts whether the total number of particles is even (+1) or odd (-1). For c 's that are periodic, the number is odd, whereas for antiperiodic c 's, this number is even.

To incorporate these two boundary conditions on the c 's, we take

$$c_j = \frac{1}{\sqrt{N}} \sum_{m=0}^{N-1} e^{i\frac{2\pi}{N}j(m+b)} \tilde{c}_m^{(b)}, \quad (13)$$

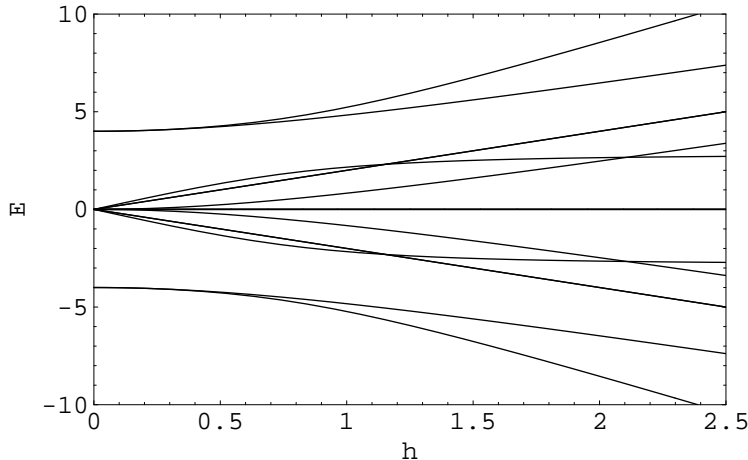


FIG. 1: Energy spectrum vs. magnetic field h for the Ising spin chain with $N = 4$ qubits from the Bogoliubov diagonalization. The results are identical to exact matrix diagonalization.

where $b = 0$ for periodic c 's; $b = 1/2$ for anti-periodic c 's. (This explains why we label the lowest two states by $|\Psi_{1/2}\rangle$ and $|\Psi_0\rangle$.) The momentum index m ranges from 0 to $N - 1$. In terms of these fermion operators the Hamiltonian becomes

$$\mathcal{H} = -Nh - \sum_{m=0}^{N-1} \left\{ \left[2 \cos \frac{2\pi}{N}(m+b) - 2h \right] \tilde{c}_m^{(b)\dagger} \tilde{c}_m^{(b)} + ir \sin \frac{2\pi}{N}(m+b) \left[\tilde{c}_m^{(b)} \tilde{c}_{N-m-2b}^{(b)} + \tilde{c}_m^{(b)\dagger} \tilde{c}_{N-m-2b}^{(b)\dagger} \right] \right\}. \quad (14)$$

Upon using the Bogoliubov transformation

$$\tilde{c}_m^{(b)} = \cos \theta_m^{(b)} \gamma_m^{(b)} + i \sin \theta_m^{(b)} \gamma_{N-m-2b}^{(b)\dagger}, \quad (15)$$

with

$$\tan 2\theta_m^{(b)} = r \sin \frac{2\pi(m+b)}{N} / \left(h - \cos \frac{2\pi(m+b)}{N} \right), \quad (16)$$

one arrives at the diagonal the Hamiltonian:

$$\mathcal{H} = -Nh + \sum_{m=0}^{N-1} \varepsilon_m^{(b)} \left(\tilde{\gamma}_m^{(b)\dagger} \tilde{\gamma}_m^{(b)} - \frac{1}{2} \right), \quad (17a)$$

$$\varepsilon_m^{(b)} = 2 \sqrt{\left(h - \cos \frac{2\pi(m+b)}{N} \right)^2 + r^2 \sin^2 \frac{2\pi(m+b)}{N}}, \quad (17b)$$

except for the special case that $\varepsilon_0^{(0)} = 2(h-1)$.

We remark that we have not left out any constant in diagonalizing the Hamiltonian in either case, so the energy spectrum is exact. For each value of b the diagonalization gives 2^N

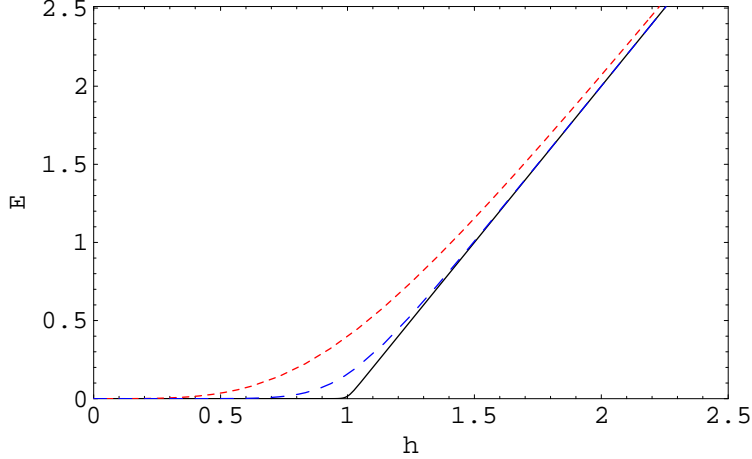


FIG. 2: (Color online) Energy gap vs. magnetic field h for the Ising spin chain with $N = 4$ (red shorter dashed), $N = 10$ (blue longer dashed), and $N = 100$ (black solid curve).

energy eigenvalues, so there are 2^{N+1} in total. Half of them are spurious. In determining the correct 2^N states from the 2^{N+1} solutions, one has to impose a constraint from the boundary conditions. Namely, in case I there can be only odd number of fermions, whereas in case II there can be only even number of fermions.

For $b = 0$, viz, the odd-number-fermion case, the lowest state $|\Psi_0\rangle$ is such that $\langle \tilde{\gamma}_m^{(0)\dagger} \tilde{\gamma}_m^{(0)} \rangle = 0$ except that $\langle \tilde{\gamma}_0^{(0)\dagger} \tilde{\gamma}_0^{(0)} \rangle = 1$. Its energy eigenvalue is

$$E_0^{(0)}(r, h) = (h - 1) - \sum_{m=1}^{N-1} \sqrt{\left(h - \cos \frac{2\pi m}{N}\right)^2 + r^2 \sin^2 \frac{2\pi m}{N}}. \quad (18)$$

For $b = 1/2$, namely, the even-number-fermion case, the lowest state $|\Psi_{1/2}\rangle$ is such that $\langle \tilde{\gamma}_m^{(1/2)\dagger} \tilde{\gamma}_m^{(1/2)} \rangle = 0$ for all m . Its eigen-energy is

$$E_0^{(1/2)}(r, h) = - \sum_{m=0}^{N-1} \sqrt{\left(h - \cos \frac{2\pi(m+1/2)}{N}\right)^2 + r^2 \sin^2 \frac{2\pi(m+1/2)}{N}}. \quad (19)$$

We see that, as $N \rightarrow \infty$, the above two energy levels are degenerate for $h \leq 1$. Furthermore, as $N \rightarrow \infty$ the difference between the two energy levels becomes

$$E_0^{(0)}(r, h) - E_0^{(1/2)}(r, h) = 2(h - 1)\Theta(h - 1), \quad (20)$$

where $\Theta(x) = 1$ if $x > 0$ and zero otherwise. The way the energy gap vanishes as $h \rightarrow 1^+$ gives a relation between two exponents

$$z\nu = 1; \quad (21)$$

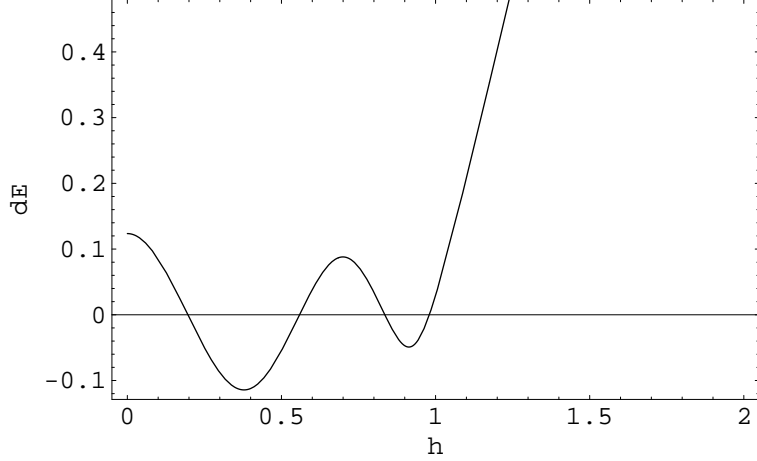


FIG. 3: Energy Energy difference $dE \equiv E_0^{(0)} - E_0^{(1/2)}$ vs. magnetic field h for the XY spin chain with $r = 0.2$ and $N = 8$ qubits from the Bogoliubov diagonalization.

z is the dynamical exponent (defined via the vanishing of energy gap $\Delta \sim |h - h_c|^{z\nu}$) and ν is the correlation-length exponent (defined via $L_c \sim |h - h_c|^{-\nu}$).

We show in Fig. 1 the energy spectrum for $N = 4$ Ising spin chain obtained from the above JW and Bogoliubov diagonalization, which is identical to direct matrix diagonalization (not shown). This means that the choice of our boundary conditions below Eq. (11) is correct. We illustrate the gap in the spectrum for the Ising chain in Fig. 2, which is obviously degenerate for $h < 1$ and linear $(h - 1)$ for $h > 1$, as derived in Eq. (20). We see that $E_0^{(0)}$ is asymptotically (i.e., as $N \rightarrow \infty$) degenerate with $E_0^{(1/2)}$ in $h \in [0, 1]$, but the former has higher energy than the latter for $h > 1$. For finite N , $E_0^{(0)}$ is larger than $E_0^{(1/2)}$. However, this is not the case for general XY model, as we illustrate in Fig. 3 for $r = 0.2$, where we see that the two branches switch roles of being the true ground state, depending on the value of h .

Even though the ground state may switch back and forth between $|\Psi_{1/2}\rangle$ and $|\Psi_0\rangle$ for $h < 1$, for $h \geq 1$ $|\Psi_{1/2}\rangle$ is the ground state. In particular, at $h = 1$ we calculate $\Delta_N(r) \equiv E_0^{(0)}(r, h = 1) - E_0^{(1/2)}(r, h = 1)$ for the finite chain with N spins and find that

$$\Delta_N(r) = \frac{\pi r}{2N} + \mathcal{O}(1/N^2). \quad (22)$$

It is interesting to see that the difference in the two energies is proportional to the anisotropy r and, as expected, inversely proportional to the system size N .

V. DERIVATION OF OVERLAP OF THE LOWEST TWO STATES WITH THE PRODUCT ANSATZ STATE

Having found the lowest two eigenstates, the quantity Λ_{\max} of Eq. (1)—and hence the entanglement—can be found, at least in principle. To do this, we parametrize the separable states via

$$|\Phi\rangle \equiv \bigotimes_{i=1}^N [\cos(\xi_i/2)|\uparrow\rangle_i + e^{i\phi_i} \sin(\xi_i/2)|\downarrow\rangle_i], \quad (23)$$

where $|\uparrow/\downarrow\rangle$ denote spin states parallel/antiparallel to the z -axis. Instead of maximizing the overlap with respect to the $2N$ real parameters $\{\xi_i, \phi_i\}$, for the lowest two states it is adequate to appeal to the translational symmetry of and the reality of the ground-state wavefunctions. Thus taking $\xi_i = \xi$ and $\phi_i = 0$ we make the Ansatz:

$$|\Phi(\xi)\rangle \equiv e^{-i\frac{\xi}{2}\sum_{j=1}^N \sigma_j^y} |\uparrow\uparrow \dots \uparrow\rangle \quad (24)$$

for searching for the maximal the overlap $\Lambda_{\max}(\Psi)$ [48]. This form shows that this separable state can be constructed as a global rotation of the ground state at $h = \infty$, viz., the separable state $|\uparrow\uparrow \dots \uparrow\rangle$. In this particular limit the boundary condition on the c 's is irrelevant, as the dominant term in the Hamiltonian is $-\sum_j h(1 - 2c_j^\dagger c_j)$.

The energy eigenstates are readily expressed in terms of the Jordan-Wigner fermion operators, and so too is the family of the Ansatz states $|\Phi(\xi)\rangle$. By working in this fermion basis we are able to evaluate the overlaps between the two lowest states and the Ansatz states, presented in the next section.

We first analyze $b = 1/2$ case, viz., the even-fermion case. The lowest state $|\Psi_{1/2}(r, h)\rangle$ has zero number of Bogoliubov fermions. It is related to the state that has no c -fermions, i.e., $|\Omega\rangle \equiv |\uparrow \dots \uparrow\rangle$ via

$$|\Psi_{1/2}(r, h)\rangle = \prod_{m=0}^{m < \frac{N-1}{2}} \cos \theta_m^{(1/2)}(r, h) e^{i \tan \theta_m^{(1/2)}(r, h) \tilde{c}_m^{(1/2)\dagger} \tilde{c}_{N-m-1}^{(1/2)\dagger}} |\Omega\rangle \quad (25a)$$

$$= \prod_{m=0}^{m < \frac{N-1}{2}} \left[\cos \theta_m(r, h) + i \sin \theta_m(r, h) \tilde{c}_m^\dagger \tilde{c}_{N-m-1}^\dagger \right] |\Omega\rangle. \quad (25b)$$

The Ansatz state is then

$$|\Phi(\xi)\rangle = \prod_{j=1}^N \left[\cos \frac{\xi}{2} + \sin \frac{\xi}{2} \prod_{1 \leq l < j} (1 - 2c_l^\dagger c_l)(c_j^\dagger - c_j) \right] |\Omega\rangle \quad (26a)$$

$$= \prod_{j=1}^N \left(\cos \frac{\xi}{2} + \sin \frac{\xi}{2} c_j^\dagger \right) |\Omega\rangle \quad (26b)$$

$$= \cos^N \frac{\xi}{2} e^{\tan \frac{\xi}{2} c_1^\dagger} \dots e^{\tan \frac{\xi}{2} c_N^\dagger} |\Omega\rangle \quad (26c)$$

$$= \cos^N \frac{\xi}{2} e^{\tan \frac{\xi}{2} \sum_{j=1}^N c_j^\dagger} e^{\tan^2 \frac{\xi}{2} \sum_{j < l} c_j^\dagger c_l^\dagger} |\Omega\rangle, \quad (26d)$$

where we have suppressed the index (1/2). The term $\sum_{j < l} c_j^\dagger c_l^\dagger$ can be rewritten in momentum space as

$$\sum_{1 \leq j < l \leq N} c_j^\dagger c_l^\dagger = i \sum_{m=0}^{m < \frac{N-1}{2}} \cot \frac{\pi(m + \frac{1}{2})}{N} \tilde{c}_m^\dagger \tilde{c}_{N-m-1}^\dagger. \quad (27)$$

Thus, for even N

$$|\Phi(\xi)\rangle = \left(1 + \tan \frac{\xi}{2} \sum_{j=1}^N c_j^\dagger \right) \prod_{m=0}^{m < \frac{N-1}{2}} \left(\cos^2 \frac{\xi}{2} + i \sin^2 \frac{\xi}{2} \cot \frac{\pi(m + \frac{1}{2})}{N} \tilde{c}_m^\dagger \tilde{c}_{N-m-1}^\dagger \right) |\Omega\rangle, \quad (28a)$$

whereas for odd N

$$|\Phi(\xi)\rangle = \left(1 + \tan \frac{\xi}{2} \sum_{j=1}^N c_j^\dagger \right) \cos \frac{\xi}{2} \prod_{m=0}^{m < \frac{N-1}{2}} \left(\cos^2 \frac{\xi}{2} + i \sin^2 \frac{\xi}{2} \cot \frac{\pi(m + \frac{1}{2})}{N} \tilde{c}_m^\dagger \tilde{c}_{N-m-1}^\dagger \right) |\Omega\rangle. \quad (28b)$$

Therefore, the overlap of the state $|\Psi_{1/2}(r, h)\rangle$ with $|\Phi(\xi)\rangle$ for even N is

$$\langle \Psi_{1/2}(r, h) | \Phi(\xi) \rangle = \prod_{m=0}^{m < \frac{N-1}{2}} \left(\cos \theta_m^{(1/2)}(r, h) \cos^2 \frac{\xi}{2} + \sin \theta_m^{(1/2)}(r, h) \sin^2 \frac{\xi}{2} \cot \frac{\pi(m + \frac{1}{2})}{N} \right), \quad (29a)$$

whereas for odd N

$$\langle \Psi_{1/2}(r, h) | \Phi(\xi) \rangle = \cos \frac{\xi}{2} \prod_{m=0}^{m < \frac{N-1}{2}} \left(\cos \theta_m^{(1/2)}(r, h) \cos^2 \frac{\xi}{2} + \sin \theta_m^{(1/2)}(r, h) \sin^2 \frac{\xi}{2} \cot \frac{\pi(m + \frac{1}{2})}{N} \right). \quad (29b)$$

Next, we discuss the $b = 0$ (odd-fermion) case. The lowest allowed state is the one with one $\gamma_0^{(0)} = \tilde{c}_0^{(0)}$ fermion:

$$|\Psi_0(r, h)\rangle \equiv \gamma_0^{(0)\dagger} |G(r, h)\rangle = \tilde{c}_0^{(0)\dagger} |G(r, h)\rangle, \quad (30)$$

where $|G(r, h)\rangle$ is the state with no γ fermions:

$$|G(r, h)\rangle = \prod_{m=1}^{m < \frac{N}{2}} \left[\cos \theta_m^{(0)}(r, h) + i \sin \theta_m^{(0)}(r, h) \tilde{c}_m^{(0)\dagger} \tilde{c}_{N-m}^{(0)\dagger} \right] |\Omega\rangle. \quad (31)$$

Similar to the $b = 1/2$ case, by using

$$\sum_{1 \leq j < l \leq N} c_j^\dagger c_l^\dagger = i \sum_{m=1}^{m < \frac{N}{2}} \cot \frac{\pi m}{N} \tilde{c}_m^{(0)\dagger} \tilde{c}_{N-m}^{(0)\dagger}, \quad (32)$$

we obtain that for even N

$$|\Phi(\xi)\rangle = \left(1 + \sqrt{N} \tan \frac{\xi}{2} \tilde{c}_0^\dagger\right) \cos^2 \frac{\xi}{2} \prod_{m=1}^{m < \frac{N}{2}} \left(\cos^2 \frac{\xi}{2} + i \sin^2 \frac{\xi}{2} \cot \frac{\pi m}{N} \tilde{c}_m^\dagger \tilde{c}_{N-m}^\dagger \right) |\Omega\rangle, \quad (33a)$$

whereas for odd N

$$|\Phi(\xi)\rangle = \left(1 + \sqrt{N} \tan \frac{\xi}{2} \tilde{c}_0^\dagger\right) \cos \frac{\xi}{2} \prod_{m=1}^{m < \frac{N}{2}} \left(\cos^2 \frac{\xi}{2} + i \sin^2 \frac{\xi}{2} \cot \frac{\pi m}{N} \tilde{c}_m^\dagger \tilde{c}_{N-m}^\dagger \right) |\Omega\rangle. \quad (33b)$$

Therefore, the overlap of $|\Psi_0(r, h)\rangle$ with $|\Phi(\xi)\rangle$ for even N is

$$\langle \Psi_0(r, h) | \Phi(\xi) \rangle = \sqrt{N} \sin \frac{\xi}{2} \prod_{m=1}^{m < \frac{N}{2}} \left(\cos \theta_m^{(0)}(r, h) \cos^2 \frac{\xi}{2} + \sin \theta_m^{(0)}(r, h) \sin^2 \frac{\xi}{2} \cot \frac{\pi m}{N} \right), \quad (34)$$

whereas for odd N

$$\langle \Psi_0(r, h) | \Phi(\xi) \rangle = \sqrt{N} \sin \frac{\xi}{2} \cos \frac{\xi}{2} \prod_{m=1}^{m < \frac{N}{2}} \left(\cos \theta_m^{(0)}(r, h) \cos^2 \frac{\xi}{2} + \sin \theta_m^{(0)}(r, h) \sin^2 \frac{\xi}{2} \cot \frac{\pi m}{N} \right). \quad (35)$$

Summarizing the above derivations: with $|\Psi_0\rangle$ ($|\Psi_{1/2}\rangle$) denoting the lowest state in the odd (even) fermion-number sector, we arrive at the overlaps

$$\langle \Psi_b(r, h) | \Phi(\xi) \rangle = f_N^{(b)}(\xi) \prod_{m=1-2b}^{m < \frac{N-1}{2}} \left[\cos \theta_m^{(b)}(r, h) \cos^2(\xi/2) + \sin \theta_m^{(b)}(r, h) \sin^2(\xi/2) \cot(k_{m,N}^{(b)}/2) \right], \quad (36)$$

with

$$k_{m,N}^{(b)} \equiv \frac{2\pi}{N}(m+b), \quad \tan 2\theta_m^{(b)}(r, h) \equiv r \sin k_{m,N}^{(b)} / (h - \cos k_{m,N}^{(b)}); \quad (37a)$$

$$f_N^{(1/2)}(\xi) \equiv 1, \quad f_N^{(0)}(\xi) \equiv \sqrt{N} \sin(\xi/2) \cos(\xi/2), \quad (N \text{ even}); \quad (37b)$$

$$f_N^{(1/2)}(\xi) \equiv \cos(\xi/2), \quad f_N^{(0)}(\xi) \equiv \sqrt{N} \sin(\xi/2), \quad (N \text{ odd}); \quad (37c)$$

where $b = 0, 1/2$ and $m \in [0, N - 1]$ is the (integer) momentum index. The above results are *exact* for arbitrary N , obtained with periodic boundary conditions on spins rather than in the so-called c -cyclic approximation [49]. Given these overlaps, we can readily obtain the entanglement of the ground state, the first excited state, and any linear superposition, $\cos \alpha |\Psi_0\rangle + \sin \alpha |\Psi_1\rangle$ of the two lowest states, for arbitrary (r, h) and N , by maximizing the magnitude of the overlap with respect to the single, real parameter ξ .

We remark that with the lowest states explicitly expressed in terms of the fermionic language, their fidelity measure [23] can be easily evaluated. Our focus here is the geometric measure of entanglement, which we derive in the next sections.

VI. ENTANGLEMENT IN THE TRANSVERSE-FIELD XY CHAINS

The formulas regarding the overlaps of $|\Psi_b\rangle$'s with product state $|\Phi(\xi)\rangle$ [in Eqs. (36) and (37)] contain all the results that we shall explore shortly, including both finite-size and infinite-size limits. By analyzing the structure of Eq. (36), we find that the global entanglement does provide information on the phase structure and critical properties of the quantum spin chains. Two of features, as captured in Figs. 4 and 5, are: (i) although the entanglement itself is, generically, not maximized at the quantum critical line in the (r, h) plane, *the field-derivative of the entanglement diverges as the critical line $h = 1$ is approached*; and (ii) the entanglement *vanishes* at the disorder line $r^2 + h^2 = 1$, which separates the oscillatory and ferromagnetic phases.

As is to be expected, at finite N the two lowest states $|\Psi_0\rangle$ (with energy $E_0^{(0)}$) and $|\Psi_{1/2}\rangle$ (with energy $E_0^{(1/2)}$) featuring in Eq. (36) do not spontaneously break the Z_2 symmetry. However, in the thermodynamic limit they are degenerate for $h \leq 1$, and linear combinations are also ground states. The question then arises as to whether linear combinations that explicitly break Z_2 symmetry, i.e., the physically relevant states with finite spontaneous magnetization, show the same entanglement properties. In fact, we see from Eq. (36) that, in the thermodynamic limit, overlaps for $|\Psi_0\rangle$ and $|\Psi_{1/2}\rangle$ are identical, up to the prefactors $f_N^{(0)}$ and $f_N^{(1/2)}$. These prefactors do not contribute to the entanglement density, and the entanglement density is therefore the same for both $|\Psi_0\rangle$ and $|\Psi_{1/2}\rangle$. It further follows that, in the thermodynamic limit, the results for the entanglement density are insensitive to the replacement of a symmetric ground state by a broken-symmetry one.

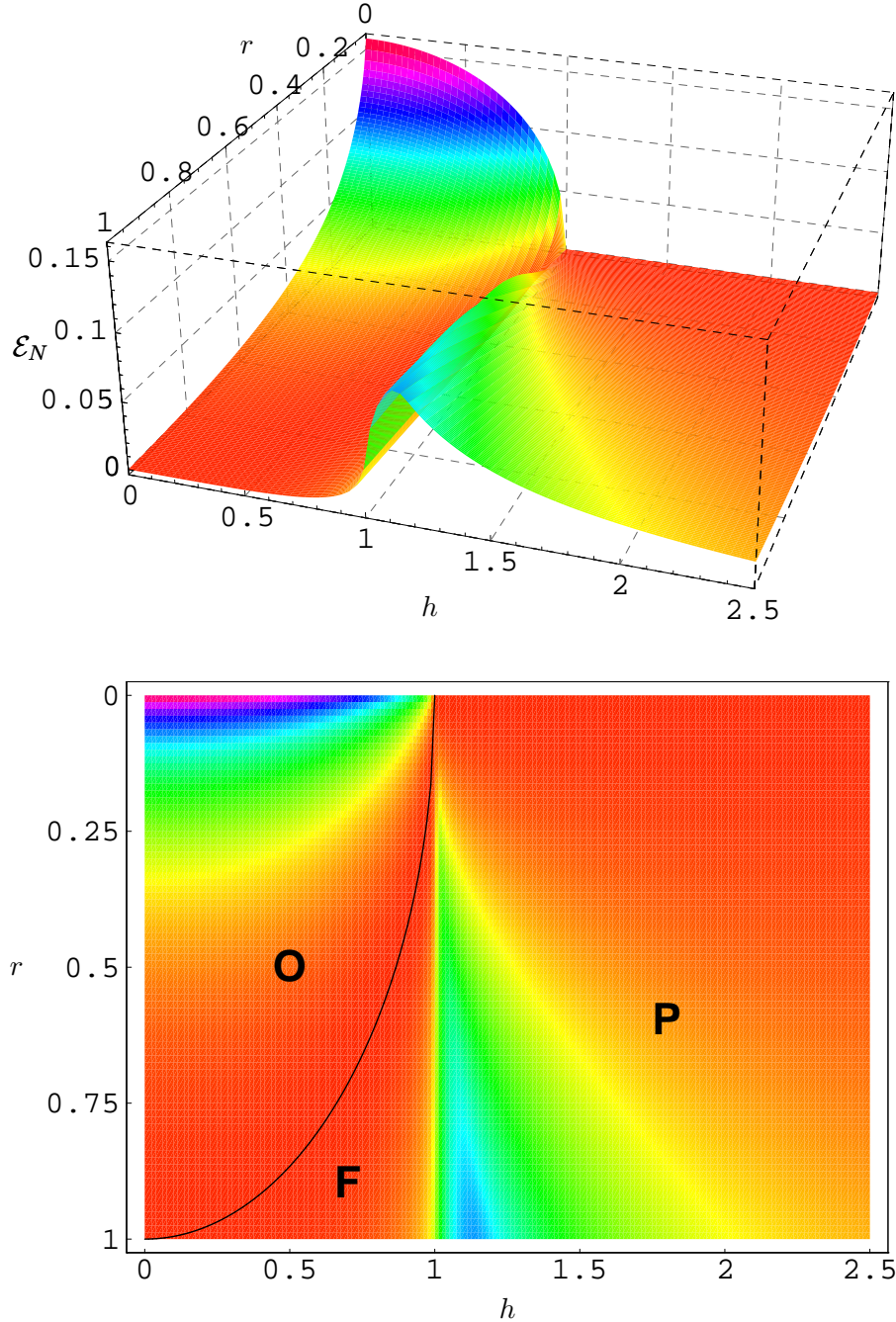


FIG. 4: (Color online) Entanglement density (upper) and phase diagram (lower) vs. (r, h) for the XY model with $N = 10^4$ spins, which is essentially in the thermodynamic limit. There are three phases: **O**: ordered oscillatory, for $r^2 + h^2 < 1$ and $r \neq 0$; **F**: ordered ferromagnetic, between $r^2 + h^2 > 1$ and $h < 1$; **P**: paramagnetic, for $h > 1$. As is apparent, there is a sharp rise in the entanglement across the line $h = 1$, which signifies a quantum phase transition. The arc $h^2 + r^2 = 1$, along which the entanglement density is zero (see also Fig. 5), separates phases **O** and **F**. Along $r = 0$ lies the XX model, which belongs to a different universality class from the anisotropic XY model.

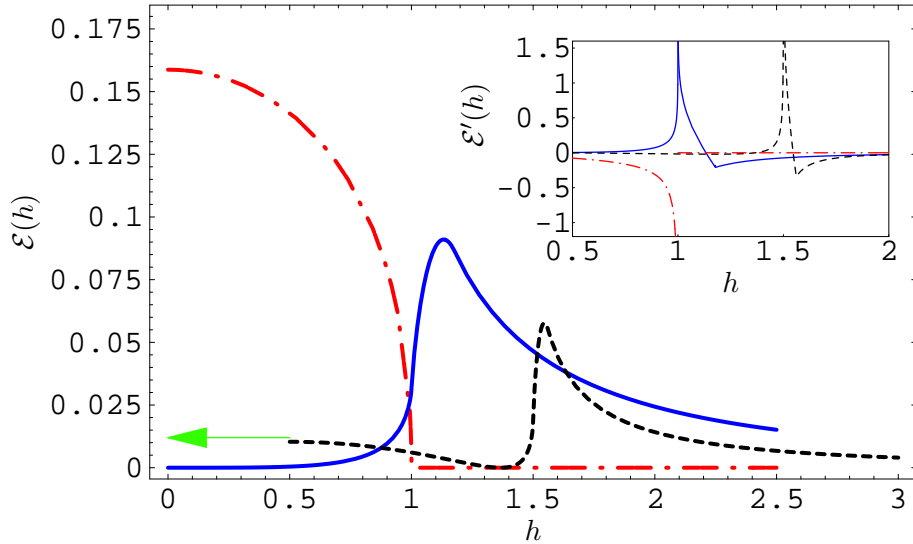


FIG. 5: (Color online) Entanglement density and its h -derivative (inset) for the ground state of three systems at $N = \infty$. Solid line: Ising ($r = 1$) limit; dashed line: anisotropic ($r = 1/2$) XY model; dash-dotted line: ($r = 0$) XX model. For the sake of clarity, the XY-case curves are shifted to the right by 0.5, indicated by the arrow. For the $r = 1/2$ case, at the entanglement density vanishes at $h = \sqrt{1 - r^2}$, which is a general property for the anisotropic XY model. Note that whilst the entanglement itself has a nonsingular maximum at $h \approx 1.1$ (Ising), $h \approx 1.04$ ($r = 1/2$ XY), and $h = 0$ (XX), respectively, it has a singularity at the quantum critical point at $h = 1$, as revealed by the divergence of its derivative.

One the other hand, entanglement of finite-size systems does depend on the exact ground state(s) and which superposition to take when there is degeneracy. For instance, the ground state switches between $|\Psi_0\rangle$ and $|\Psi_{1/2}\rangle$ (see Fig. 3), and the ground-state entanglement for a finite system can be broken into pieces (see Fig. 8). Furthermore, we shall also investigate the entanglement of the superposition: $\cos\theta|\Psi_{1/2}\rangle + \sin\theta|\Psi_0\rangle$.

A. Entanglement for finite spins

Before we discuss the thermodynamic limit of the entanglement density, we compare the entanglement obtained via the results in Eq. (36) and that obtained via numerically diagonalizing the Hamiltonian and calculating the maximal overlap. In Figure 6 the results via each method are shown for the Ising case ($r = 1$) with small numbers of spins ($N = 13$

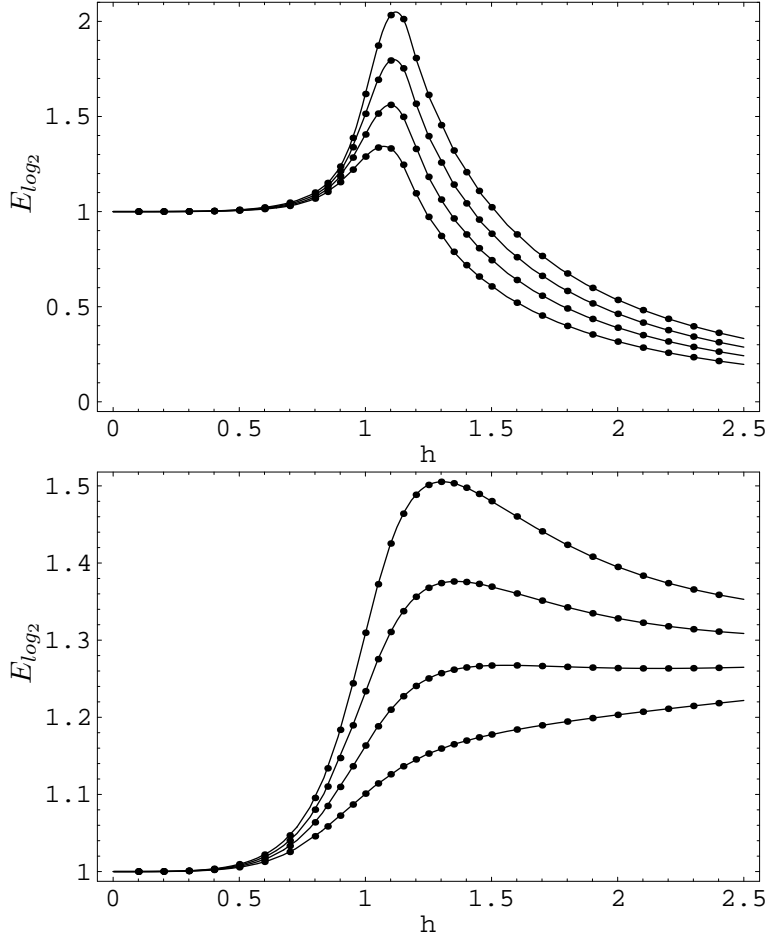


FIG. 6: Total entanglement vs. magnetic field h for ground (upper panel) and first excited (lower panel) states with small $N = 13, 16, 19, 22$ (from bottom to top) for the transverse Ising model ($r = 1$). The numerical results are shown as discrete points whereas the analytical results are shown as lines. This demonstrates that the analytical results are exact, even for small N , both even and odd.

through 22), it is seen that our analytical results are exact even for small N , both even and odd.

As another example, we show in Fig. 7 the total entanglement for the ground state of the XX chain with $N = 100$ spins. The entanglement varies with h stepwise. This makes sense as at $h = 0$, the ground state has continuous symmetry in XY plane, and hence has high entanglement. As h increases, the z-component total angular momentum increases by one once the increase exceeds certain threshold, breaking the continuous symmetry, and hence the entanglement decreases stepwise until at $h = 1$ when all the spins are pointing in the

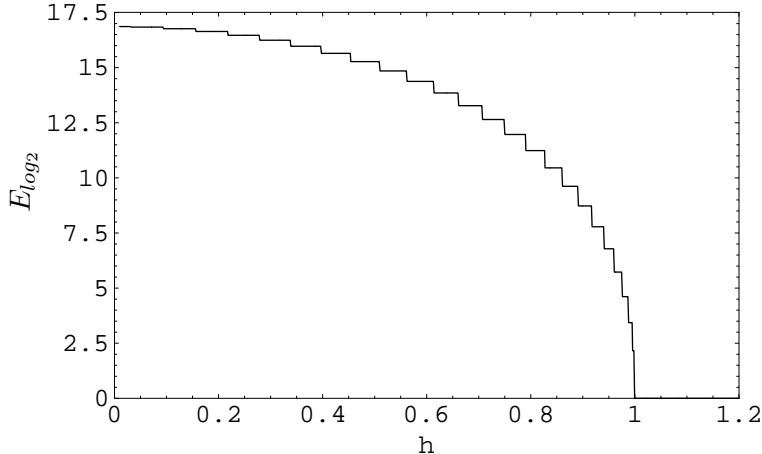


FIG. 7: Total entanglement vs. magnetic field h for the ground state of XX chain with $N = 100$ qubits.

z-direction. In the limit $N \rightarrow \infty$ the change in the step per spin becomes infinitesimal and the curve becomes smooth shown in Fig. 5 as expected.

As a final example in this section, we illustrate the strange feature of piecewise continuity for finite-system ground-state entanglement. Take $r = 0.2$ and $N = 8$ for example. The ground state switch between the two states labeled by the energy $E_0^{(0)}$ (odd fermion number) and $E_0^{(1/2)}$ (even fermion number), as already shown in Fig. 3. In Fig. 8, we show the entanglement for these two states (solid red and dashed blue dashed curves), as well as the ground-state entanglement obtained from exact diagonalization (shown as dots). The ground state for this system has a piecewise continuity in its entanglement. A similar behavior has also been observed in the context of the hierarchical geometric entanglement [45, 46]. We remark that when one considers the entanglement per site, the difference between the entanglement density of the two states vanishes in the thermodynamic limit, as we shall see below.

B. Entanglement density of infinite chains

From Eq. (36) it follows that the thermodynamic limit of the entanglement density is given by

$$\mathcal{E}(r, h) = -\frac{2}{\ln 2} \max_{\xi} \int_0^{\frac{1}{2}} d\mu \ln [\cos \theta(\mu, r, h) \cos^2(\xi/2) + \sin \theta(\mu, r, h) \sin^2(\xi/2) \cot \pi \mu], \quad (38)$$

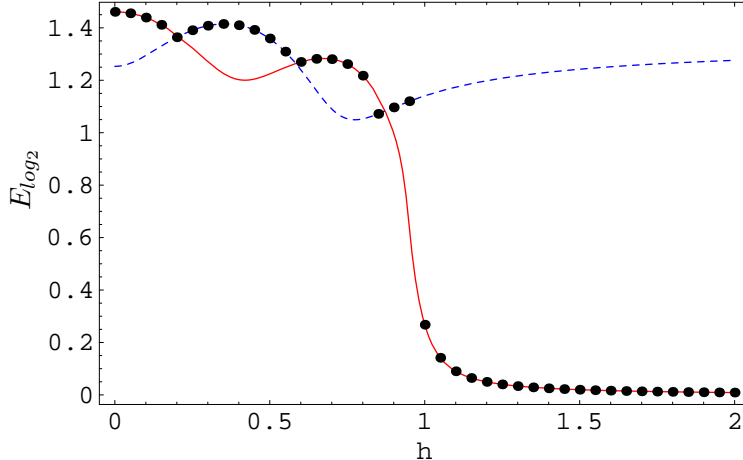


FIG. 8: (Color online) Total entanglement vs. magnetic field h of the XY chain with $r = 0.2$ and $N = 8$ for the ground state (black dots), the minimum energy state in odd-fermion sector $E_0^{(0)}$ (dashed blue curve) and even-fermion sector $E_0^{(1/2)}$ (solid red). We see that the ground state, and hence its entanglement, switches between these two states; see also Fig. 3.

where $\tan 2\theta(\mu, r, h) \equiv r \sin 2\pi\mu / (h - \cos 2\pi\mu)$.

Figure 5 shows the thermodynamic limit of the entanglement density $\mathcal{E}(r, h)$ and its h -derivative in the ground state, as a function of h for three values of r , i.e., three slices through the surface shown in Fig. 4. As the $r = 1$ slice shows, in the Ising limit the entanglement density is small for both small and large h . It increases with h from zero, monotonically, albeit very slowly for small h , then swiftly rising to a maximum at $h \approx 1.13$ before decreasing monotonically upon further increase of h , asymptotically to zero. The entanglement maximum *does not* occur at the quantum critical point. However, the derivative of the entanglement with respect to h *does* diverge at the critical point $h = 1$, as shown in the inset. The slice at $r = 1/2$ (for clarity, shifted half a unit to the right) shows qualitatively similar behavior, except that it is finite (although small) at $h = 0$, and starts out by decreasing to a shallow minimum of zero at $h = \sqrt{1 - r^2}$. By contrast, the slice at $r = 0$ (XX) starts out at $h = 0$ at a maximum value of $1 - 2\gamma_C / (\pi \ln 2) \approx 0.159$. (where $\gamma_C \approx 0.9160$ is the *Catalan* constant), the globally maximal value of the entanglement over the entire (r, h) plane. For larger h it falls monotonically until it vanishes at $h = 1$, remaining zero for larger h .

Let us analyze the behavior of the entanglement derive for $r \neq 0$ (Ising universality class) case first.

1. *Divergence of entanglement-derivative for the anisotropic XY models*

The starting point is Eq. (38), in which there is a maximization over the variable ξ . The function to be maximized is

$$F(\xi, r, h) \equiv \int_0^{\frac{1}{2}} d\mu \ln [\cos \theta(\mu, r, h) \cos^2(\xi/2) + \sin \theta(\mu, r, h) \sin^2(\xi/2) \cot \pi\mu]. \quad (39)$$

To find the stationarity condition, we demand the derivative with respect to ξ vanishes ($\partial_\xi F(\xi, r, h)|_{\xi=\xi^*} = 0$), where

$$\partial_\xi F(\xi, r, h)|_{\xi=\xi^*} = -\frac{1}{2} \sin \xi \int_0^{\frac{1}{2}} d\mu \frac{\cos \theta(\mu, r, h) - \sin \theta(\mu, r, h) \cot \pi\mu}{\cos \theta(\mu, r, h) \cos^2(\xi/2) + \sin \theta(\mu, r, h) \sin^2(\xi/2) \cot \pi\mu} \Big|_{\xi=\xi^*}. \quad (40)$$

Denote by $\xi^*(h)$ the solution for fixed r . Then the field-derivative of the entanglement is

$$\partial_h \mathcal{E}(r, h) = \frac{-2}{\ln 2} \partial_h F(\xi^*(h), h) = \frac{-2}{\ln 2} \left[\frac{\partial \xi^*(h)}{\partial h} \partial_\xi F(\xi, h) \Big|_{\xi^*} + \partial_h F(\xi^*, h) \right] = \frac{-2}{\ln 2} \partial_h F(\xi^*, h), \quad (41)$$

where the first term in the square bracket vanishes identically due to the condition (40).

Thus (dropping the * on ξ for convenience),

$$\partial_h \mathcal{E}(r, h) = -\frac{2}{\ln 2} \partial_h F(\xi^*, h) \quad (42)$$

$$= -\frac{2}{\ln 2} \int_0^{\frac{1}{2}} d\mu \frac{\partial_h \cos \theta(\mu, r, h) \cos^2(\xi/2) + \partial_h \sin \theta(\mu, r, h) \sin^2(\xi/2) \cot \pi\mu}{\cos \theta(\mu, r, h) \cos^2(\xi/2) + \sin \theta(\mu, r, h) \sin^2(\xi/2) \cot \pi\mu}. \quad (43)$$

Recall that $\tan 2\theta(\mu, r, h) \equiv r \sin 2\pi\mu / (h - \cos 2\pi\mu)$ and thus

$$\cos \theta = \sqrt{(1 + \cos 2\theta)/2}, \quad \sin \theta = \sqrt{(1 - \cos 2\theta)/2}, \quad (44a)$$

$$\cos 2\theta(\mu, r, h) = \frac{h - \cos 2\pi\mu}{\sqrt{(r \sin 2\pi\mu)^2 + (h - \cos 2\pi\mu)^2}}. \quad (44b)$$

Putting everything in Eq. (43), we get

$$\begin{aligned} \partial_h \mathcal{E}(r, h) &= -\frac{r}{\ln 2} \int_0^{\frac{1}{2}} d\mu \frac{\sin 2\pi\mu}{(r \sin 2\pi\mu)^2 + (h - \cos 2\pi\mu)^2} \\ &\quad \frac{\sqrt{\sqrt{\quad} - (h - \cos 2\pi\mu) \cos^2(\xi/2)} - \sqrt{\sqrt{\quad} + (h - \cos 2\pi\mu) \sin^2(\xi/2) \cot \pi\mu}}{\sqrt{\sqrt{\quad} + (h - \cos 2\pi\mu) \cos^2(\xi/2)} + \sqrt{\sqrt{\quad} - (h - \cos 2\pi\mu) \sin^2(\xi/2) \cot \pi\mu}} \end{aligned} \quad (45)$$

where $\sqrt{\quad} \equiv \sqrt{(r \sin 2\pi\mu)^2 + (h - \cos 2\pi\mu)^2}$.

We aim to explore the behavior near $h = 1$. First consider $h > 1$ and define $\epsilon \equiv h - 1$, which is the deviation from the critical point. Make the change of variables $t = h - \cos 2\pi\nu$,

giving lower and upper limits ϵ and $2 + \epsilon$, respectively. We further shift the integration variable by ϵ , arriving at

$$\begin{aligned} \partial_h \mathcal{E}(r, h) = & -\frac{r}{2\pi \ln 2} \int_0^2 dt \frac{1}{(1-r^2)t^2 + 2(r^2 + \epsilon)t + \epsilon^2} \\ & \frac{\sqrt{t} \sqrt{\sqrt{\quad} - (t + \epsilon) \cos^2(\xi/2)} - \sqrt{\sqrt{\quad} + (t + \epsilon) \sin^2(\xi/2)} \sqrt{2-t}}{\sqrt{t} \sqrt{\sqrt{\quad} + (t + \epsilon) \cos^2(\xi/2)} + \sqrt{\sqrt{\quad} - (t + \epsilon) \sin^2(\xi/2)} \sqrt{2-t}}, \end{aligned} \quad (46)$$

where $\sqrt{\quad} = \sqrt{(1-r^2)t^2 + 2(r^2 + \epsilon)t + \epsilon^2}$.

As we inspect the limit $h \rightarrow 1$ or $\epsilon \rightarrow 0$, we see that the above expression diverges, with the contribution coming from t small, i.e., infrared divergence. Large $t (\leq 2)$ does not contribute to the divergence. Note further that only the second term in the numerator contributes to the divergence. We then proceed to evaluate the integral by separating it into two parts:

$$\int_0^2 = \int_0^\delta + \int_\delta^2, \quad (47)$$

with $\delta \ll 1$. In the first region we only need to keep t to first order at most. Also noting that for $t, \epsilon \ll 1$, the first term in the denominator is much smaller than the second term, we get

$$-\frac{r}{2\pi \ln 2} \int_0^\delta dt \frac{-1}{2r^2(t + \frac{\epsilon^2}{2r^2})} \frac{\sqrt{\sqrt{2(r^2 + \epsilon)t + \epsilon^2} + (t + \epsilon)}}{\sqrt{\sqrt{2(r^2 + \epsilon)t + \epsilon^2} - (t + \epsilon)}}. \quad (48)$$

Next, we simplify the second term (ignoring ϵ when there is no danger in doing so)

$$\frac{\sqrt{\sqrt{2(r^2 + \epsilon)t + \epsilon^2} + (t + \epsilon)}}{\sqrt{\sqrt{2(r^2 + \epsilon)t + \epsilon^2} - (t + \epsilon)}} = \frac{\sqrt{t + \frac{\epsilon^2}{2r^2}}}{\sqrt{t}} + \frac{t + \epsilon}{\sqrt{2r^2 t}}. \quad (49)$$

Observing that only the first term on the right-hand side contributes to the divergence, we have that the divergent part is

$$-\frac{r}{2\pi \ln 2} \int_0^\delta dt \frac{-1}{2r^2(t + \frac{\epsilon^2}{2r^2})} \frac{\sqrt{t + \frac{\epsilon^2}{2r^2}}}{\sqrt{t}} = \frac{1}{4r\pi \ln 2} \int_0^{\delta 2r^2/\epsilon^2} dt \frac{1}{\sqrt{t+1}} \frac{1}{\sqrt{t}}. \quad (50)$$

The divergence part is then (for $\delta 2r^2/\epsilon^2 \gg 1$)

$$\frac{1}{4r\pi \ln 2} 2 \sinh^{-1} \sqrt{\delta 2r^2/\epsilon^2} \approx \frac{1}{2r\pi \ln 2} \ln \left(2\sqrt{\delta 2r^2/\epsilon^2} \right) = -\frac{1}{2r\pi \ln 2} \ln \epsilon + \frac{\ln(2\sqrt{\delta 2r^2})}{2r\pi \ln 2}. \quad (51)$$

As the integral (46) does not depend on the choice of δ , the part that involves δ must be cancelled by the second half of the integration \int_{δ}^2 , which can be verified by direct evaluation. Therefore, for h very close to $h_c = 1$, we have

$$\frac{\partial \mathcal{E}}{\partial h} \approx -\frac{1}{2\pi r \ln 2} \ln |h - 1|. \quad (52)$$

In deriving the above divergence form, we have assumed that $r \neq 0$. Similar consideration can be applied to the case when h approaches 1 from below, and the behavior is the same.

2. Divergence of entanglement-derivative for the XX limit of the model

We now analyze the $r = 0$ isotropic (XX universality class) case. It turns out that the analysis for this case is much simpler. To see this, we first note when $r = 0$ we have the simplification

$$\cos 2\theta(\mu, h) = \text{sgn}(h - \cos 2\pi\mu). \quad (53)$$

The above expression changes sign when $h = \cos 2\pi\nu$. So let us introduce the variable $\mu_0 \equiv (\cos^{-1} h)/(2\pi)$. The expression for the entanglement density Eq. (38) becomes

$$\mathcal{E}(h) - \frac{2}{\ln 2} \max_{\xi} \int_0^{\frac{1}{2}} d\mu \ln [\cos \theta(\mu, r, h) \cos^2(\xi/2) + \sin \theta(\mu, r, h) \sin^2(\xi/2) \cot \pi\mu] \quad (54a)$$

$$= -\frac{2}{\ln 2} \max_{\xi} \left[\int_0^{\mu_0} d\mu \ln \sin^2(\xi/2) \cot \pi\mu + \int_{\mu_0}^{\frac{1}{2}} d\mu \ln \cos^2(\xi/2) \right]. \quad (54b)$$

Demanding stationarity with respect to ξ gives the condition

$$[\mu_0 - \frac{1}{4}(1 - \cos \xi)] \sin \xi = 0. \quad (55)$$

The solution $\xi = 0$ gives the entanglement density for $h \geq 1$. It is straightforward to see from Eq. (54a) that the entanglement density is identically zero. The solution $\mu_0 - \frac{1}{4}(1 - \cos \xi) = 0$ gives

$$\cos \xi = 1 - \frac{2}{\pi} \cos^{-1} h. \quad (56)$$

This in turn gives the entanglement density for $0 \leq h \leq 1$:

$$\mathcal{E}(h) = -\frac{2}{\ln 2} \left[\mu_0(h) \ln \frac{2\mu_0(h)}{1 - 2\mu_0(h)} + \frac{1}{2} \ln(1 - 2\mu_0(h)) + \int_0^{\mu_0(h)} d\mu \ln \cot \pi\mu \right]. \quad (57)$$

Thus we have derived the entanglement density as a function of the magnetic field h in the XX limit. The result is shown in Fig. (5).

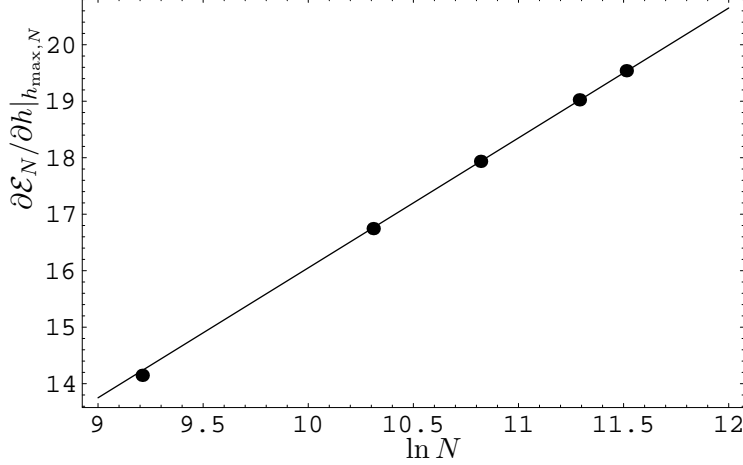


FIG. 9: Finite-size scaling. $\partial \mathcal{E}_N / \partial h|_{h_{\max, N}}$ vs. $\ln N$, for $N = 10^4, 3 \times 10^4, 5 \times 10^4, 8 \times 10^4$, and 10^5 (points) with $r = 0.1$. The solid line represents the fit $\partial \mathcal{E}_N / \partial h|_{h_{\max, N}} \approx 2.30 \ln N - 6.95$.

We see from the figure that the entanglement density at $h = 0$ is the highest, which being $\mathcal{E}(0) = 1 - 2\gamma_C / (\pi \ln 2) \approx 0.159$ by evaluating Eq. (57) at $h = 0$. The constant $\gamma_C \approx 0.9160$ is the *Catalan* constant. The entanglement density decreases monotonically as h increases until $h = 1$ beyond which it becomes zero identically. This qualitative behavior can be understood as follows. As the total z -component spin is conserved, increasing h simply increases the z -component spin of the ground state until $h = 1$ where all the spins are aligned with the field, hence there is no entanglement beyond this value of h .

By directly taking the derivative with respect to h , we get

$$\partial_h \mathcal{E}(h) = \frac{1}{\pi \ln 2 \sqrt{1-h^2}} \ln \left[\frac{\cos^{-1} h}{\pi - \cos^{-1} h} \sqrt{\frac{1+h}{1-h}} \right]. \quad (58)$$

Near $h \approx 1$, we have (putting $1+h=2$ and evaluating the limit in the argument of log function)

$$\frac{\partial}{\partial h} \mathcal{E}(0, h) \approx -\frac{\log_2(\pi/2)}{\sqrt{2}\pi} \frac{1}{\sqrt{1-h}}, \quad (h \rightarrow 1^-). \quad (59)$$

This completes our derivation of the singular behavior of the entanglement density near the critical points.

3. Singularity of entanglement and quantum criticality

Let us summarize the above derivations of the singular behavior in the entanglement density and discuss the connection to quantum criticality, in particular the correlation length

critical exponent.

(1) The singular behavior of the field-derivative of the entanglement density (38) in the vicinity of the quantum critical line acts as (for $r \neq 0$)

$$\frac{\partial \mathcal{E}}{\partial h} \approx -\frac{1}{2\pi r \ln 2} \ln |h - 1|, \text{ for } |h - 1| \ll 1. \quad (60)$$

From the arbitrary- N results (36) of the entanglement we analyze the approach to the thermodynamic limit, in order to develop further connections with quantum criticality. We focus on the exponent ν , which governs the divergence at criticality of the correlation length: $L_c \sim |h - 1|^{-\nu}$. To do this, we compare the divergence of the slope $\partial \mathcal{E}_N / \partial h$ (i) near $h = 1$ (at $N = \infty$), given above, and (ii) for large N at the value of h for which the slope is maximal (viz. $h_{\max, N}$), i.e., $\partial \mathcal{E}_N / \partial h|_{h_{\max, N}} \approx 0.230r^{-1} \ln N + \text{const.}$, obtained by analyzing Eq. (36) for various values of r ; see Fig. 9 for the example of $r = 0.1$ case. Then, noting that $(2\pi \ln 2)^{-1} \approx 0.2296$ and that the logarithmic scaling hypothesis [50] (or see Appendix A) identifies ν with the ratio of the amplitudes of these divergences, $0.2296/0.230 \approx 1$, we recover the known result that $\nu = 1$. Moreover, from Eq. (21) we can extract the value of the dynamical exponent: $z = 1$.

(2) Compared with $r \neq 0$ case, the nature of the divergence of $\partial \mathcal{E} / \partial h$ at $r = 0$ belongs to a different (XX) universality class:

$$\frac{\partial}{\partial h} \mathcal{E}(0, h) \approx -\frac{\log_2(\pi/2)}{\sqrt{2}\pi} \frac{1}{\sqrt{1-h}}, \quad (h \rightarrow 1^-). \quad (61)$$

From this divergence, the scaling hypothesis, and the assumption that the entanglement density is intensive, we can infer the known result [12] that the critical exponent $\nu = 1/2$ for the XX model. Moreover, from Eq. (21) we can extract the value of the dynamical exponent $z = 2$ for the XX model.

In keeping with the critical features of the XY-model phase diagram, for any small but nonzero value of the anisotropy, the critical divergence of the entanglement derivative is governed by Ising-type behavior. It is only at the $r = 0$ point that the critical behavior of the entanglement is governed by the XX universality class. For small r , XX behavior ultimately crosses over to Ising behavior.

C. Vanishing of entanglement density along the disorder line

We find that along the line $r^2 + h^2 = 1$ the entanglement density vanishes in the thermodynamic limit. In fact, this line exactly corresponds to the boundary separating the oscillatory and ferromagnetic phases; the boundary can be characterized by a set of ground states with total entanglement of order unity, and thus of zero entanglement density. The entanglement density is also able to track the phase boundary ($h = 1$) between the ordered and disordered phases. Associated with the quantum fluctuations accompanying the transition, the entanglement density shows a drastic variation across the boundary and the field-derivative diverges all along $h = 1$. The two boundaries separating the three phases coalesce at $(r, h) = (0, 1)$, i.e., the XX critical point. Figures 4 and 5 reveal all these features.

One extreme limit is the Ising case, i.e., $r = 1$ and $h = 0$, where the ground state is either $|\rightarrow\rightarrow\cdots\rightarrow\rangle$ or $|\leftarrow\leftarrow\cdots\leftarrow\rangle$, both of these being unentangled. Any superposition of them is also a valid ground state, but it has entanglement of order unity. In the thermodynamic limit the entanglement per spin is identically zero. Is this a general feature along the disorder line? Before we establish this, recall that the energies of the lowest two levels are given in Eqs. (18) and (19). Evaluating them at $r^2 = 1 - h^2$, we immediately find that both are $-N$.

Now let us evaluate the expectation value of the Hamiltonian (4) with respect to a separable state with all spins pointing in the same direction:

$$\langle \mathcal{H} \rangle = -N \left(\frac{1+r}{2} \langle \sigma^x \rangle^2 + \frac{1-r}{2} \langle \sigma^y \rangle^2 + h \langle \sigma^z \rangle \right). \quad (62)$$

Denoting $x \equiv \langle \sigma^x \rangle$, $y \equiv \langle \sigma^y \rangle$, $z \equiv \langle \sigma^z \rangle$, we find that the above expression achieves its minimum value $-N$ at $r^2 + h^2 = 1$ when

$$(x, y, z) = \left(\pm \sqrt{\frac{2r}{1+r}}, 0, \sqrt{\frac{1-r}{1+r}} \right). \quad (63)$$

Therefore, the separable state satisfying the above conditions is the ground state, and there is a degeneracy. Hence, along the disorder line the total entanglement can be at most of order unity (due to superposition of the above degenerate states) and hence the entanglement density vanishes. We note that the theory of factorized ground states has recently been extensively developed and greatly understood [16, 51, 52], and it turns out that they occur quite often and their occurrence is related to the existence of quantum critical points nearby in the system parameter.

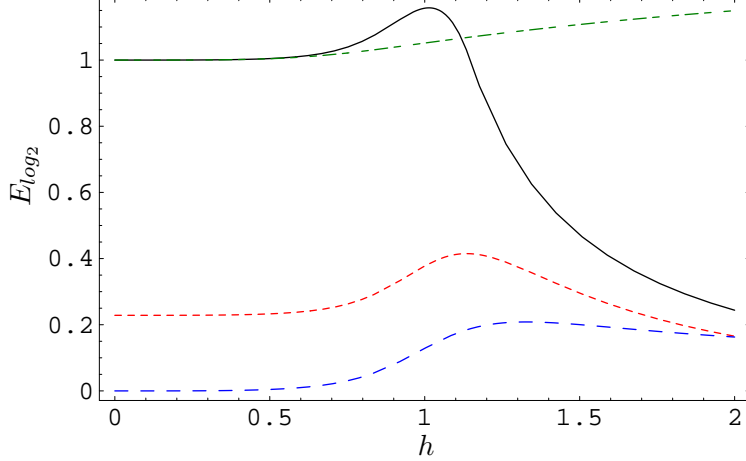


FIG. 10: (Color online) Total entanglement (E_{\log_2}) for an Ising chain vs. the field h for $N = 10$ and various superposition of $\cos \theta |\Psi_{1/2}\rangle + \sin \theta |\Psi_0\rangle$: $\theta = 0$ (solid black), $\theta = \pi/8$ (short-dashed red), $\theta = \pi/4$ (long-dashed blue), and $\theta = \pi/2$ (mixed-dashed green).

D. Entanglement of superposition

In this section, we discuss the entanglement of superposition for the two lowest states $|\Psi_{1/2}\rangle$ and $|\Psi_0\rangle$:

$$|\Psi(r, h, \theta)\rangle = \cos \theta |\Psi_{1/2}(r, h)\rangle + \sin \theta |\Psi_0(r, h)\rangle. \quad (64)$$

Why does this interest us? Take for instance the Ising model, $r = 1$. The states $|\Psi_{1/2}\rangle$ and $|\Psi_0\rangle$, respectively, analytically continues to (as $h \rightarrow 0$)

$$|\Psi_{1/2}(1, 0)\rangle = (|\rightarrow\rightarrow\cdots\rightarrow\rangle + |\leftarrow\leftarrow\cdots\leftarrow\rangle)/\sqrt{2} \quad (65a)$$

$$|\Psi_0(1, 0)\rangle = (|\rightarrow\rightarrow\cdots\rightarrow\rangle - |\leftarrow\leftarrow\cdots\leftarrow\rangle)/\sqrt{2}. \quad (65b)$$

This is a result of unbroken Z_2 symmetry and both states possess global geometric entanglement of unity. In the large system size limit, this symmetry is usually broken due to fluctuations of a random magnetic field, and the resulting symmetry-broken states will be unentangled, having zero entanglement. These symmetry-broken states can be represented as certain superposition of the original symmetry-unbroken states. But to evaluate the entanglement for these symmetry-broken states at a different field value h , we need to be able to calculate the entanglement of the superposition, shown in the above equations.

Fortunately, we have already evaluated the overlap of the two states with the same product state $|\Phi(\xi)\rangle$, as summarized in Eqs. (36) and (37). We only need to compute the

sum of the two overlaps weighted by the coefficients $\cos \theta$ and $\sin \theta$ and maximize the norm of the overlap with respect to the parameter ξ . As an illustration, we have computed the entanglement of superposition for the Ising model with $N = 10$ spins, as shown in Fig. 10. The resultant entanglement does depend on the detail of the superposition.

The above exercise can be generalized to all values of r , h , and N , including the infinite limit. If we are interested only in the entanglement per spin, it is now readily easy to see from Eq. (36) that, in the thermodynamic limit, overlaps for $|\Psi_0\rangle$ and $|\Psi_{1/2}\rangle$ are identical, up to the prefactors $f_N^{(0)}$ and $f_N^{(1/2)}$. These prefactors do not contribute to the entanglement density (although they do matter for the correction in $1/N$), and the entanglement density is therefore the same for both $|\Psi_0\rangle$ and $|\Psi_{1/2}\rangle$. It further follows that, in the thermodynamic limit, the results for the entanglement density are insensitive to the replacement of a symmetric ground state by a broken-symmetry one.

E. Finite-size scaling of entanglement at critical points

Recall that we have performed a finite-size scaling of the entanglement derivative in Sec. VIB3 in order to extract the critical exponent for the Ising universality class. What about the finite-size scaling of the entanglement density itself near criticality? This question was recently raised and addressed by Shi and co-workers [53], and they have found a scaling of the entanglement per site \mathcal{E}_N as

$$\mathcal{E}_N \sim \mathcal{E}_\infty + \frac{b}{N} + \frac{c}{N^2}. \quad (66)$$

With the formulas of entanglement given above, we can address this question straightforwardly. But as we have discussed earlier, the correction to the entanglement may depend on which superposition of degenerate states we use. To avoid the ambiguity, we present the finite-size scaling at $h = 1$ for both states $|\Psi_{1/2}\rangle$ (which is the ground state at $h = 1$) and $|\Psi_0\rangle$ at various values of $r \neq 0$. We shall see that although their \mathcal{E}_∞ 's are practically the same, the scaling coefficients b and c are different. One interesting observation is that (for $r \neq 0$) we obtain $b \approx 1.0$ for $|\Psi_{1/2}\rangle$ and $b \approx 0.5$ for $|\Psi_0\rangle$. The correction b/N has recently been shown to related to the Affleck-Ludwig boundary entropy by Stéphan and co-workers [54]. Furthermore, c is negative for $|\Psi_{1/2}\rangle$ and positive for $|\Psi_0\rangle$. (For $r = 0$ XX model at $h = 1$, the entanglement density is identically zero. There is no need to per-

r	$ \Psi_{1/2}\rangle$			$ \Psi_0\rangle$		
	\mathcal{E}_∞	b	c	\mathcal{E}_∞	b	c
0.1	0.00426345	1.00266	-10.6643	0.00425344	0.512785	17.5478
0.2	0.00817338	1.00038	-5.39161	0.00817141	0.502356	10.1401
0.3	0.0117754	1.00013	-3.73401	0.0117747	0.500874	7.23486
0.4	0.0151133	1.00006	-2.91527	0.0151129	0.500444	5.71366
0.5	0.0182208	1.00004	-2.42561	0.0182206	0.500268	4.78119
0.6	0.0211258	1.00002	-2.09918	0.0211256	0.500181	4.15147
0.7	0.0238512	1.00002	-1.86569	0.0238511	0.500131	3.6975
0.8	0.0264164	1.00001	-1.69019	0.0264163	0.500101	3.35452
0.9	0.0288377	1.00001	-1.55332	0.0288376	0.50008	3.08608
1.0	0.0311291	1.00001	-1.44349	0.031129	0.500066	2.87013

TABLE I: Table for the scaling parameters \mathcal{E}_∞ , b , and c at various r but at fixed $h = 1$ for $|\Psi_{1/2}\rangle$ and $|\Psi_0\rangle$. The results are obtained from fitting the number of spins N from 100 to 1000.

form the finite-size scaling.) To get the scaling fit, we use the size N from 100 to 1000, and calculate the respective entanglement for fitting Eq. (66). The results are tabulated in Table I. Curiously, the c 's for $|\Psi_{1/2}\rangle$ are approximately half and negative of those for $|\Psi_0\rangle$, i.e., $c^{(1/2)} \approx -c^{(0)}/2$.

VII. CONCLUDING REMARKS

In summary, we have quantified the global entanglement of the quantum XY spin chain. This model exhibits a rich phase structure, the qualitative features of which are reflected by this entanglement measure. Perhaps the most interesting aspect is the divergence in the field-derivative of the entanglement as the critical line ($h = 1$) is crossed. The behavior of the divergence is dictated by the universality class of the model. Furthermore, in the thermodynamic limit, the entanglement density vanishes on the disorder line ($r^2 + h^2 = 1$). The structure of the entanglement surface, as a function of the parameters of the model (the magnetic field h and the coupling anisotropy r), is surprisingly rich. We have also discussed issues of superposition of entanglement, its independence on the spontaneous breaking of

the Z_2 symmetry, and finite-size scaling at critical points

How does ground-state entanglement reflect quantum phase transitions? Can we have a generic understanding of the connection? Near quantum critical points, the correlation length generally scales as

$$\xi(h) \sim |h - h_c|^{-\nu}, \quad (67)$$

with ν denoting the so-called correlation-length exponent. For any density functions, such as free energy density and the entanglement density, we expect scaling for the singular part behaves as (e.g. Ref. [55])

$$\mathcal{E}(h) \sim (\xi/a)^{-d} (c_1 + c_2 \log(\xi/a) + \dots), \quad (68)$$

where d is the dimension of the system, a is the smallest length scale, c 's are some constants which may depend on which side of critical point we are at, and we have included a possible logarithmic correction in its simplest form. The idea is that near criticality the only length scale is the correlation length, and any density quantity should scale as 1/volume, i.e., $1/(\xi/a)^d$, with a being a unit of length. We then expect that in general

$$\left. \frac{d\mathcal{E}(h)}{dh} \right|_{h_c^\pm} \sim \pm a^d |h - h_c|^{d\nu-1} (\tilde{c}_1 + \tilde{c}_2 \log |h - h_c|). \quad (69)$$

For the one-dimensional ($d = 1$) Ising universality class, $\nu = 1$, and there is a logarithmic divergence, which is consistent with Eq. (60). For the XX universality near $h = 1$, there is no logarithmic correction (i.e., $c_2 = \tilde{c}_2 = 0$), the correlation length exponent $\nu = 1/2$. The resultant divergence from the above scaling form is consistent with what we have obtained in Eq. (59), noting that the coefficient $c_1 = 0$ for $h > h_c$.

We close by pointing towards a deeper connection between the global measure of entanglement and the correlations among quantum fluctuations. The maximal overlap (1) can be decomposed in terms of correlation functions:

$$\Lambda_{\max}^2 = \frac{1}{2^N} + \frac{N}{2^N} \max_{|\vec{r}|=1} \left\{ \langle \vec{r} \cdot \vec{\sigma}_1 \rangle + \frac{1}{2} \sum_{j=2}^N \langle \vec{r} \cdot \vec{\sigma}_1 \otimes \vec{r} \cdot \vec{\sigma}_j \rangle + \dots \right\},$$

where translational invariance is assumed and the Cartesian coordinates of \vec{r} can be taken to be $(\sin \xi, 0, \cos \xi)$. The two-point correlations appearing in the decomposition are related to a bi-partite measure of entanglement, namely, the concurrence, which shows similar singular behavior [7] to Eq. (60).

In fact, it was elaborated in Ref. [35] that a singularity of the entanglement can come from two types of sources: (i) correlation functions, $\mathcal{C}_{[i,j,k,\dots]}^{\alpha,\beta,\gamma,\dots} \equiv \langle \sigma_{[i]}^\alpha \sigma_{[j]}^\beta \sigma_{[k]}^\gamma \dots \rangle$ for the ground state $|\Psi\rangle$, and (ii) parameters $\vec{r}^{*[i]}$, which denote the vectors that maximize the overlap. For transverse Ising, which has a standard second-order quantum critical point, (i) correlation functions \mathcal{C} 's are singular but (ii) optimal parameters r^* 's are not singular and this explains the similar behavior between the GE and the concurrence. It can happen that the singularity of the entanglement near a transition can come from different types. In Ref. [35], it was realized that near the so-called Kosterlitz-Thouless point (the isotropic antiferromagnetic point) of the XXZ model, the correlation length is finite, but (ii) r^* 's are singular. It is this second point the one that detects non-analyticity in the wavefunction across the transition.

Acknowledgments—The authors acknowledge many valuable discussions with D. Das, S. Mukhopadhyay, and R. Orús. This work was supported by NSERC and MITACS (TCW), by NSF DMR-0644022-CAR (SV) and by the U.S. Department of Energy, Division of Materials Sciences under Award No. DE-FG02-07ER46453, through the Frederick Seitz Materials Research Laboratory at the University of Illinois at Urbana-Champaign (PMG).

Appendix A: Finite-size scaling

The discussion here follows Barber [50]. In the vicinity of the bulk critical temperature T_C the behavior of a system should depend on $y \equiv L/\xi(T)$, where $\xi(T)$ is the bulk correlation length and L is the characteristic length of the system. How does the divergence of certain thermodynamic quantities emerge as the system size L grows?

1. Algebraic divergence

Assume that some thermodynamic quantity at $L \rightarrow \infty$ diverges as $t \equiv (T - T_C)/T_C \rightarrow \infty$:

$$P_\infty(T) \sim C_\infty t^{-\rho}. \quad (\text{A1})$$

Finite-size scaling hypothesis asserts that for finite L and T near T_C ,

$$P_L(T) \sim l^\omega Q_P(l^{1/\nu} \tilde{t}), \quad l \rightarrow \infty, \quad \tilde{t} \rightarrow 0, \quad (\text{A2})$$

where $l \equiv L/a$ (a is some microscopic length), $\tilde{t} \equiv [T - T_C(L)]$. The exponent ω can be determined by the requirement that the $P_L(T)$ reproduces $P_\infty(T)$ as $l \rightarrow \infty$. Thus,

$$Q_P(x) \sim C_\infty x^{-\rho}, \quad x \rightarrow \infty, \quad (\text{A3})$$

and $\omega = \rho/\nu$. We consider the case that the finite system does not exhibit a true transition, then

$$Q_P(x) \rightarrow Q_0, \quad x \rightarrow 0. \quad (\text{A4})$$

From this we have that at the peak or rounding temperature $T_m^*(l)$ (where P_L reaches the maximum or deviates significantly from the bulk value)

$$P_L(T_m^*(l)) \sim Q_0 l^{\rho/\nu}, \quad l \rightarrow \infty. \quad (\text{A5})$$

This means that the behavior of a thermodynamic quantity varies with the system size is determined by the bulk critical exponent.

2. Logarithmic divergence

Now assume the thermodynamic quantity $P(T)$ diverges logarithmically as

$$P_\infty(T) \sim C_\infty \ln t, \quad t \rightarrow 0, \quad (\text{A6})$$

as in the field-derivative of the entanglement density for anisotropic XY spin chains. The finite-size scaling hypothesis in this case is to assume

$$P_L(T) - P_L(T_0) \sim Q_P(l^{1/\nu} \tilde{t}) - Q_P(l^{1/\nu} \tilde{t}_0), \quad (\text{A7})$$

where T_0 is some non-critical temperature and $\tilde{t}_0 \equiv (T_0 - T_C(L))/T_C$. The hypothesis has to recover the $l \rightarrow \infty$ limit at fixed T , which requires

$$Q_P(x) \sim C_\infty \ln x, \quad x \rightarrow \infty. \quad (\text{A8})$$

Thus in the limit $\tilde{t} \rightarrow 0$ at fixed large l , we have

$$P_L(T_C(L)) \sim -\frac{C_\infty}{\nu} \ln l + O(1), \quad (\text{A9})$$

if $Q_P(x) = O(1)$ as $x \rightarrow 0$. This allows us to obtain the exponent ν by analyzing how the divergence develops as the system size l (which is N in our spin-chain entanglement problem) increases.

-
- [1] C. H. Bennett, G. Brassard, C. Crépeau, R. Jozsa, A. Peres, and W. K. Wootters, Phys. Rev. Lett. **70**, 1895 (1993).
 - [2] C. H. Bennett and S. J. Wiesner, Phys. Rev. Lett. **69**, 2881 (1992).
 - [3] A. K. Ekert, Phys. Rev. Lett. **67**, 661 (1991).
 - [4] M. Nielsen and I. Chuang, *Quantum Computation and Quantum Information* (Cambridge Univ. Press, 2000).
 - [5] L. Amico, R. Fazio, A. Osterloh, and V. Vedral, Rev. Mod. Phys. **80**, 517 (2008).
 - [6] T. J. Osborne and M. A. Nielsen, Phys. Rev. A **66**, 032110 (2002).
 - [7] A. Osterloh, L. Amico, G. Falci, and R. Fazio, Nature **416**, 608 (2002).
 - [8] G. Vidal, J. I. Latorre, E. Rico, and A. Kitaev, Phys. Rev. Lett. **90**, 227902 (2003).
 - [9] P. Calabrese, J. Cardy, JSTAT 0406:002 (2004).
 - [10] V. E. Korepin, Phys. Rev. Lett. **92** 096402 (2004).
 - [11] H. Barnum, G. Ortiz, R. Somma, and L. Viola, Phys. Rev. Lett. **92**, 107902 (2004).
 - [12] S. Sachdev, *Quantum phase transitions* (Cambridge University Press, 1999).
 - [13] C. N. Yang and C. P. Yang, Phys. Rev. **150**, 327 (1966).
 - [14] It can happen that too much entanglement may not be useful, see, e.g., D. Gross, S. T. Flammia, and J. Eisert, Phys. Rev. Lett. **102**, 190501 (2009); M. J. Bremner, C. Mora, and A. Winter, Phys. Rev. Lett. **102**, 190502 (2009).
 - [15] M. B. Plenio and S. Virmani, Quantum Inf. Comput. **7**, 1 (2007). R. Horodecki, P. Horodecki, M. Horodecki, and K. Horodecki, Rev. Mod. Phys. **81**, 865 (2009).
 - [16] T. Roscilde, P. Verrucchi, A. Fubini, S. Haas, and V. Tognetti, Phys. Rev. Lett. **93**, 167203 (2004).
 - [17] M.-C. Chung and I. Peschel, Phys. Rev. B **64**, 064412 (2001).
 - [18] V. E. Korepin, Phys. Rev. Lett. **92** 096402 (2004); A. R. Its, B. Q. Jin, V. E. Korepin, Journal Phys. A: Math. Gen. **38**, 2975-2990, (2005). M. B. Plenio, J. Eisert, J. Dreissig, M. Cramer, Phys. Rev. Lett. **94** 060503 (2005); M. M. M. Wolf, Phys. Rev. Lett. **96**, 010404 (2006).

- J. Eisert, M. Cramer, Phys. Rev. A **72**, 042112 (2005); I. Peschel, J. Zhao, JSTAT P11002 (2005); R. Orús, J. I. Latorre, J. Eisert, M. Cramer, Phys. Rev. A **73**, 060303(R) (2006); A. Riera, J. I. Latorre, Phys. Rev. A **74** 052326 (2006).
- [19] W. K. Wootters, Phys. Rev. Lett. **80**, 2245 (1998).
- [20] L.-A. Wu, M. S. Sarandy, D. A. Lidar, Phys. Rev. Lett. **93**, 250404 (2004); L.-A. Wu, M. S. Sarandy, D. A. Lidar, L. J. Sham, Phys. Rev. A **74**, 052335 (2006); L. Campos Venuti, C. Degli Esposti Boschi, M. Roncaglia, A. Scaramucci, Phys. Rev. A **73**, 010303(R) (2006).
- [21] A. Wong and N. Christensen, Phys. Rev. A **63**, 044301 (2001).
- [22] M.-F. Yang, Phys. Rev. A **71**, 030302 (R) (2005).
- [23] P. Zanardi and N. Paunković, Phys. Rev. E **74**, 031123 (2006). H.-Q. Zhou and J. P. Barjaktarevic, arXiv:cond-mat/0701608v1. P. Buonsante and A. Vezzani, Phys. Rev. Lett. **98**, 110601 (2007). P. Zanardi, P. Giorda, and M. Cozzini, Phys. Rev. Lett **99**, 100603 (2007). H.-Q. Zhou, R. Orús, and G. Vidal, Phys. Rev. Lett. **100**, 080601 (2008). S. J. Gu, H.-M. Kwok, W.-Q. Ning, and H.-Q. Lin, Phys. Rev. B **77**, 245109 (2008). S. J. Gu, Int. J. Mod. Phys. B **24**, 4371 (2010).
- [24] N. Lambert, C. Emary, and T. Brandes, Phys. Rev. Lett. **92**, 073602 (2004).
- [25] S.-J. Gu, S.-S. Deng, Y.-Q. Li, and H.-Q. Lin, Phys. Rev. Lett. **93**, 086402 (2004).
- [26] D. Gioev and I. Klich, Phys. Rev. Lett. **96**, 100503 (2006).
- [27] F. Verstraete, M. Popp, and J. I. Cirac, Phys. Rev. Lett. **92**, 027901 (2004). F. Verstraete, M. A. Martin-Delgado, and J. I. Cirac, Phys. Rev. Lett. **92**, 087201 (2004).
- [28] T.-C. Wei, D. Das, S. Mukhopadyay, S. Vishveshwara, and P. M. Goldbart, Phys. Rev. A **71**, 060305 (R) (2005); T.-C. Wei, Chapter 5, Ph.D Thesis, University of Illinois (2004).
- [29] T.-C. Wei and P. M. Goldbart, Phys. Rev. A **68**, 042307 (2003).
- [30] A. Shimony, Ann. N. Y. Acad. Sci. **755**, 675 (1995).
- [31] H. Barnum and N. Linden, J. Phys. A **34**, 6787 (2001).
- [32] F. T. Arecchi, E. Courtens, R. Gilmore, and H. Thomas, Phys. Rev. A **6**, 2211 (1972).
- [33] D. C. Brody and L. P. Hughston, J. Geom. Phys. **38**, 19 (2001).
- [34] R. Orús, S. Dusuel, J. Vidal, Phys. Rev. Lett. **101**, 025701 (2008).
- [35] R. Orús and T.-C. Wei, Phys. Rev. B **82**, 155120 (2010).
- [36] R. Orús, Phys. Rev. Lett. **100**, 130502 (2008); A. Botero and B. Reznik, arXiv:0708.3391; R. Orús, Phys. Rev. A **78**, 062332 (2008).

- [37] T.-C. Wei, Phys. Rev. A **81**, 062313 (2010).
- [38] W. Son, L. Amico, S. Pascazio, R. Fazio, and V. Vedral, e-print arXiv:1001.2656v1.
- [39] C.-Y. Huang and F.-L. Lin, Phys. Rev. A **81**, 032304 (2010).
- [40] O. Biham, M. A. Nielsen, and T. J. Osborne, Phys. Rev. A **65**, 062312 (2002).
- [41] E_{\log_2} provides a lower bound to another multipartite measure: the relative entropy of entanglement, proposed by V. Vedral, M. B. Plenio, M. A. Rippin, and P. L. Knight, Phys. Rev. Lett. **78**, 2275 (1997). For further discussion, see T.-C. Wei, M. Ericsson, P. M. Goldbart, and W. J. Munro, Quantum Inf. Comput. **4**, 252 (2004); T.-C. Wei, Phys. Rev. A **78**, 012327 (2008).
- [42] T.-C. Wei, Phys. Rev. A **81**, 054102 (2010).
- [43] Y. Shimoni and O. Biham, Phys. Rev. A. **75**, 022308 (2007).
- [44] M. Blasone, F. Dell'Anno, S. De Siena, and F. Illuminati, Phys. Rev. A **77**, 062304 (2008).
- [45] M. Blasone, F. Dell'Anno, S. De Siena, S. M. Giampaolo, and F. Illuminati, J. Phys.: Conf. Ser. **174**, 012064 (2009).
- [46] M. Blasone, F. Dell'Anno, S. De Siena, S. M. Giampaolo, and F. Illuminati, Physica Scripta **T140**, 014016 (2010).
- [47] M. Henkel, *Conformal Invariance and Critical Phenomena* (Springer, 1999).
- [48] We have confirmed this Ansatz numerically for small numbers of spins.
- [49] E. Lieb, T. Schultz, and D. Mattis, Ann. Phys. **60**, 407 (1961).
- [50] M. N. Barber, in *Phase Transitions and Critical Phenomena*, Vol. 8, p. 161, Eq. (3.20), C. Domb and J. L. Lebowitz (eds.) (Academic, London, 1983).
- [51] S. J. Kurmann, H. Thomas, and G. Müller, Physica (Amsterdam) **112A**, 235 (1982). T. Roscilde, P. Verrucchi, A. Fubini, S. Hass, and V. Tognetti, Phys. Rev. Lett. **94**, 147208 (2005). R. Rossignoli, N. Canosa, and J. M. Matera, Phys. Rev. A **80**, 062325 (2009).
- [52] S. M. Giampaolo, G. Adesso, and F. Illuminati, Phys. Rev. Lett. **100**, 19721 (2008). S. M. Giampaolo, G. Adesso, and F. Illuminati, Phys. Rev. B **79**, 224434 (2009).
- [53] Q.-Q. Shi, R. Orus, J. O. Fjærrestad, H.-Q. Zhou, New J. Phys. **12**, 025008 (2010).
- [54] J.-M. Stéphan, G. Misguich, and F. Alet, Phys. Rev. B **82**, 180406 (R) (2010).
- [55] N. Goldenfeld, *Lectures on Phase Transitions and the Renormalization Group*, Addison-Wesley (Reading, Massachusetts, 1992).